



PERGAMON

Available online at [www.sciencedirect.com](http://www.sciencedirect.com)

SCIENCE @ DIRECT®

Vision Research 43 (2003) 1387–1396

Vision  
Research[www.elsevier.com/locate/visres](http://www.elsevier.com/locate/visres)

# Short-latency ocular following in humans is dependent on absolute (rather than relative) binocular disparity

D.-S. Yang <sup>a,b</sup>, F.A. Miles <sup>a,\*</sup><sup>a</sup> *Laboratory of Sensorimotor Research, National Eye Institute, National Institutes of Health, Building 49, Room 2A50, 49 Convent Drive, Bethesda, MD 20892-4435, USA*<sup>b</sup> *Department of Ophthalmology, Columbus Children's Hospital, Columbus, OH 43205, USA*

Received 16 December 2002; received in revised form 3 March 2003

## Abstract

A previous study showed that the initial ocular following responses elicited by sudden motion of a large random-dot pattern were only modestly attenuated when that whole pattern was shifted out of the plane of fixation by altering its horizontal binocular disparity, but the same disparity applied to a restricted region of the dots had a much more powerful effect [Vision Research 41 (2001) 3371]. Thus, if the dots were partitioned into horizontal bands, for example, and alternate bands were moved in opposite directions to the left or right then ocular following was very weak, but if the (conditioning) dots moving in one direction were all shifted out of the plane of fixation (by applying horizontal disparity to them) then strong ocular following was now seen in the direction of motion of the (test) dots in the plane of fixation, i.e., moving images became much less effective when they were given binocular disparity. We sought to determine if the greater impact of disparity with the partitioned images was because there were additional *relative disparity* cues. We used a similar partitioned display and found that the dependence of ocular following on the absolute disparity of the conditioning stimulus had a Gaussian form with an *x*-offset that was close to zero disparity and, importantly, this offset was almost unaffected by changing the absolute disparity of the test stimulus. We conclude from this that it is the absolute—rather than the relative—disparity that is important, and that ocular following has a strong preference for moving images whose absolute disparities are close to zero. This is consistent with the idea that ocular following selectively stabilizes the retinal images of objects in and around the plane of fixation and works in harmony with disparity vergence, which uses absolute disparity to bring objects of interest into the plane of fixation [Archives of Ophthalmology 55 (1956) 848].

© 2003 Elsevier Science Ltd. All rights reserved.

**Keywords:** Optokinetic eye movements; Binocular disparity; Visual motion; Motion segmentation

## 1. Introduction

An observer who undergoes linear motion and looks off to one side experiences motion parallax as the images of objects at different distances move across his/her retina at different speeds. In order to stabilize the retinal images of objects in the passing scene the observer must track them with his/her eyes, but if the tracking mechanism is to respond selectively to the retinal motion of the object(s) of regard in the plane of fixation then it must ignore the retinal motion of other objects that are

less or more distant. Mackensen (1953) showed that the optokinetic responses (OKN) elicited by wide-field motion were attenuated if the observer's eyes were not correctly converged or focused on the moving display, and Howard and Gonzalez (1987) confirmed this observation, suggesting that at least some part of the effect was due to the disparity of the retinal images and that the motion detectors mediating OKN were disparity selective, preferring images with zero disparity, i.e., images in the plane of fixation. In support of this idea they showed that when the display was segregated into central and peripheral regions, in which the images moved in opposite directions and one or the other was given horizontal disparity, the associated optokinetic responses were always in the direction of the binocularly fused display, whether that was peripheral or central. In a subsequent study, Howard and Simpson

\* Corresponding author. Address: Laboratory of Sensorimotor Research, National Eye Institute, National Institutes of Health, Building 49, Room 2A50, 49 Convent Drive, Bethesda, MD 20892-4435, USA. Tel.: +1-301-496-2455; fax: +1-301-402-0511.

E-mail address: [fam@sr.nei.nih.gov](mailto:fam@sr.nei.nih.gov) (F.A. Miles).

(1989) provided subjects with a vertical line on which to converge their eyes and found that the optokinetic responses elicited by vertical motion of a display made up of oblique lines were roughly inversely proportional to the horizontal disparity of the display, at least over the range examined. Masson, Busetini, Yang, and Miles (2001) reported that the initial open-loop ocular following responses (OFR) elicited by motion of a large random-dot pattern were only weakly sensitive to disparity that was applied uniformly to the whole pattern. These initial OFR are reflex-like, with ultra-short latencies of <60 ms in monkeys (Miles, Kawano, & Optican, 1986) and <80 ms in humans (Gellman, Carl, & Miles, 1990), and it has been suggested that they occur before the subject has had time to direct his/her attention to a particular part of the display and before the subject is even aware that there has been a visual disturbance (Miles, 1998). Masson et al. (2001) argued that applying the disparity uniformly to the whole moving image effectively simulated the visual experience of the rotating—rather than translating—observer who compensates only partially for the rotation and has a vergence error that renders the entire scene disparate (though normally not uniformly so): such visual disturbances lack the motion parallax associated with linear motion in a world with 3-D structure and hence lack the problem—conflicting motions in different depth planes—that binocular disparity had been hypothesized to resolve (in favor of the motion in the plane of fixation). To simulate the hypothesized motion parallax, these workers recorded the initial OFR elicited when the random-dot pattern was partitioned into two interleaved sets of horizontal bands that suddenly underwent opposite horizontal motion. This approach uncovered powerful effects of disparity on initial ocular following: when one set of (conditioning) dots was given disparity OFR now strongly favored the motion of the other set of (test) dots that lacked disparity. There were two important technical details in this study. First, the disparity was applied to the conditioning bands during a centering saccade because these workers had found that any sudden disturbances of the large-field pattern—regardless of whether they resulted in a change in disparity—produced a powerful transient suppression of OFR, an effect described previously by Kawano and Miles (1986) in monkeys. Second, the OFR stimuli—opposite motion of the test and conditioning bands—were applied soon after the saccade ended (in some cases, as early as 10 ms) to take advantage of post-saccadic enhancement, whereby motion in the immediate wake of a saccade across a textured background generates much stronger OFR than the same stimuli applied later (Gellman et al., 1990), and to preclude the possibility that there would be time for disparity-vergence eye movements to modify the applied disparity (Busettini, FitzGibbon, & Miles, 2001), or for the sub-

ject to selectively redirect his/her attention to the (test) pattern in the plane of fixation.

Masson et al. (2001) suggested that the greater dependence of OFR on disparity when the visual stimulus was partitioned into regions with conflicting motion might indicate that the motion detectors driving OFR were more sensitive to relative motion and/or relative disparity than to en masse motion and/or absolute disparity. Absolute disparity refers to the slight differences in the positions of the two retinal images of a given object resulting from the differing viewpoints of the two eyes, and relative disparity refers to the differences in the absolute disparities of different objects within the visual scene resulting from differences in their distance to the observer. In the present study we used the partitioned display of Masson et al. (2001) and sought to determine whether the disparity involved was relative and/or absolute. To obtain definitive evidence for relative disparity it is necessary to show that the disparity tuning in one region is dependent on the disparity in another region. We now report that the absolute disparity at which the conditioning stimulus has its maximal impact on OFR is little affected by changing the absolute disparity of the test stimulus, i.e., the responses to the test and conditioning stimuli are separable, hence it is the absolute and not the relative disparity of the motion stimuli that determines their impact on OFR.

## 2. Methods

The visual display, eye-movement recording techniques, experimental procedures and data analyses were very similar to those used for Experiment 3 in the paper of Masson et al. (2001) and, therefore, will only be described in brief here.

### 2.1. Subjects

Four subjects (FM, DY, BS, NB) participated. All were experienced in eye movement recordings, with stereoacuties better than 40 s of arc (Titmus test) and no known oculomotor or visual problems other than refractive errors that were corrected with spectacles (FM). Subjects BS and NB were unaware of the purpose of the experiment.

### 2.2. Visual display

The subject faced a translucent tangent screen (80° wide, 50° high, at a viewing distance of 33.3 cm) onto which four photographic images, each filling the screen, were back-projected independently. Pairs of mirror galvanometers with an X/Y configuration were positioned in each of the four light paths to provide computer control of the horizontal and vertical positions of

the images. The images were arranged in two matching dichoptic pairs, one pair forming a *test* pattern and the other pair a *conditioning* pattern. An orthogonal arrangement of polarizing filters in the projection paths and in front of the subject's eyes ensured that each eye saw only one of the two test patterns and one of the two conditioning patterns: dichoptic stimulation. The test images consisted of white dots (diameters,  $1.5^\circ$ ) arranged randomly within horizontal bands (each  $\sim 3.5^\circ$  high) distributed at vertical intervals of  $\sim 7^\circ$  on a black background (so that adjacent bands were separated by  $\sim 3.5^\circ$ ). At the start of the trial, the two test images overlapped exactly so as to create a single binocular image in the plane of the screen. The two conditioning images, which were identical to the test images except for being inverted vertically and horizontally, were also initially overlapping so as to create a single binocular image in the plane of the screen and were positioned so as to exactly fill the spaces between the bands of dots making up the test pattern. A cartoon showing the layout of the binocular images of the interleaved test and conditioning patterns can be seen in Fig. 5 of Masson et al. (2001). The bands were always vertically positioned so that a test band was at the center of the screen.

### 2.3. Eye-movement recording

The horizontal and vertical positions of both eyes were recorded with an electromagnetic induction technique (Robinson, 1963) using scleral search coils embedded in silastin rings (Collewijn, Van Der Mark, & Jansen, 1975). The outputs from the coils were calibrated at the beginning of each recording session by having the subject fixate small target lights located at known eccentricities along the horizontal and vertical meridians.

### 2.4. Procedures

The presentation of stimuli, and the acquisition, display and storage of data were controlled by a PC (Pentium II) using a real-time experimentation software package (REX) developed by Hays, Richmond, and Optican (1982).

At the beginning of each trial, the test and conditioning patterns were imaged in the plane of the screen (each dichoptic pair overlapped exactly) and were stationary for a minimum period in excess of 1 s to allow adequate time for the subject to acquire a convergent state appropriate for the near viewing (33.3 cm). During a  $10^\circ$  leftward centering saccade—guided by target spots projected onto the display—horizontal step displacements (transition time,  $\sim 2$  ms) were applied symmetrically to the image pairs to alter the horizontal disparity of the test and conditioning patterns independently. The

magnitude and polarity (i.e., crossed or uncrossed) of these disparity steps were selected randomly from two lookup tables. The table entries for the conditioning pattern were  $0^\circ$ ,  $0.4^\circ$ ,  $0.8^\circ$ ,  $1.6^\circ$ ,  $2.4^\circ$ ,  $3.2^\circ$ , and  $6.4^\circ$  and for the test pattern were  $0^\circ$  and  $1.6^\circ$ . Note that all disparities given in this paper are with respect to the center of the tangent screen unless specifically stated otherwise. Fifty milliseconds after the end of the centering saccade there was an equal probability that the test and conditioning bands would either remain stationary or undergo equal but opposite horizontal motion ( $40^\circ/\text{s}$ ) with the test bands moving leftward while the conditioning bands moved rightward, or vice versa, for 200 ms: OFR stimulus. After this, the images on the screen were blanked for 500 ms, marking the end of the trial. Each block of trials had 117 randomly interleaved stimulus combinations: 13 conditioning disparities, 3 test disparities, 3 velocities. The subject's task was to make the leftward centering saccade and then refrain from making any further saccades until the end of the trial. Subjects were given no instructions in regard to the disparity or OFR stimuli. If there were no saccades (other than the centering saccade), then the data were stored on a hard disk; otherwise, the trial was aborted and subsequently repeated. Data were collected over several sessions until each condition had been repeated an adequate number of times to permit good resolution of the responses (through averaging) even when exploring the limit of the responsive range with stimuli of marginal efficacy (actual numbers will be given in Section 3).

### 2.5. Data analysis

The horizontal and vertical eye position data obtained during the calibration procedure were each fitted with a third-order polynomial which was then used to linearize the horizontal and vertical eye position data recorded during the experiment proper. The latter were then smoothed with a cubic spline of weight  $10^7$ , selected by means of a cross-validation procedure (Eubank, 1988), and all subsequent analyses utilized these splined data. Rightward eye movements were defined as positive. The horizontal version position was computed by averaging the horizontal positions of the two eyes, and the horizontal vergence position was computed from the difference in the horizontal positions of the two eyes, left eye minus right, so that increases in the vergence angle were positive. Version and vergence velocity were obtained by two-point backward differentiation of their respective position data. Trials with saccadic intrusions were deleted. Mean version and vergence temporal profiles (position and velocity) were computed for all the data obtained for each of the 117 stimulus conditions. The initial horizontal OFR were quantified by measuring the change in horizontal version position over the 83-ms time period commencing 85 ms after the onset of

the stimulus ramps. We then computed the means of these change-in-version-position measures for each stimulus condition. The minimum latencies of onset were 85–90 ms so that these response measures were restricted to the period prior to the closure of the visual feedback loop (i.e., twice the reaction time): initial open-loop responses. To eliminate the (slight) effects due to post-saccadic drift, for each combination of test and conditioning disparities, the mean change-in-version-position measures recorded during the no-motion (saccade-only control) trials were subtracted from the same measures recorded during the motion stimulus (experimental) trials. As previously described by Masson et al. (2001), the disparity tuning curves describing the dependence of the initial OFR measures on the disparity of the conditioning stimulus were approximately bell shaped, and we fitted each with the following Gaussian function:

$$A + g \frac{e^{-(d_c - \mu)^2 / (2\sigma^2)}}{\sigma\sqrt{2\pi}} \quad (1)$$

where  $A$  is the  $y$ -offset,  $g$  is a scale factor,  $\sigma$  is the width,  $\mu$  is the  $x$ -offset, and  $d_c$  is the disparity applied to the conditioning bands. All units are degrees, except for  $g$ , which is dimensionless.

### 3. Results

#### 3.1. Sample data from one subject

Disparity tuning curves describing the dependence of the initial OFR—given by the change-in-version-position measures (see Section 2)—on the absolute disparity applied to the conditioning bands,  $d_c$ , had the roughly bell-shaped form described by Masson et al. (2001). Sample tuning curves from one subject (DY) are shown in Fig. 1. For the data in this figure, the test bands always moved leftwards while the conditioning bands always moved rightwards and, because we adopted the convention that rightward OFR are positive, OFR in the direction of the conditioning bands are plotted above zero and OFR in the direction of the test bands are plotted below zero. The data shown in filled squares were obtained while the test bands were imaged in the plane of the screen, i.e., no disparity was applied to the test bands ( $d_t = 0$ ), a situation that exactly simulated one of the stimulus configurations used by Masson et al. and essentially replicated their findings: when the conditioning bands were imaged in the plane of the screen, OFR were close to zero—actually favoring the motion in the test bands very slightly in this instance—and applying a few degrees of disparity to the conditioning bands, whether crossed or uncrossed, reduced the efficacy of the motion in those bands so that OFR now

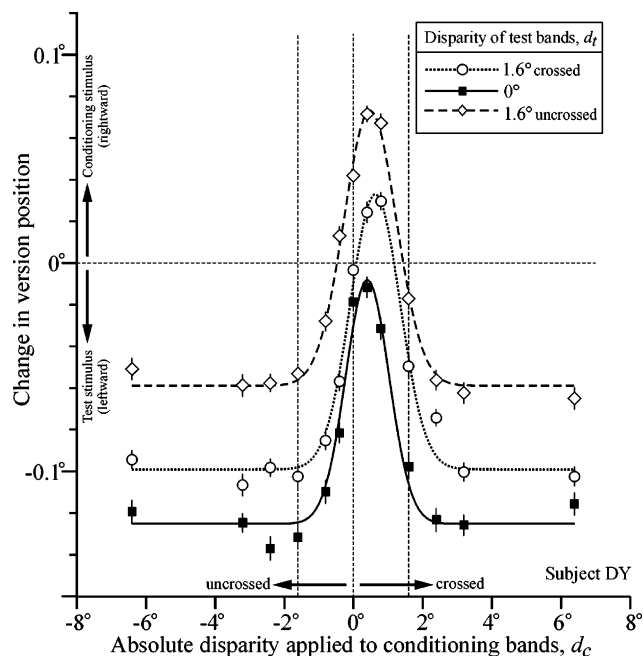


Fig. 1. Disparity tuning curves describing the dependence of OFR on the absolute disparity applied to the conditioning bands ( $d_c$ ): effects of changing the absolute disparity of the test bands ( $d_t$ ). The mean change in horizontal version position (in degrees) over the 83-ms time period starting 85 ms after the onset of the OFR stimuli is plotted against the disparity of the conditioning bands (in degrees). The test stimulus motion was leftward and the conditioning stimulus motion was rightward. The disparity of the test bands was zero (filled squares), 1.6° crossed (open circles), and 1.6° uncrossed (open diamonds). Curves are least-squares best-fitting Gaussian functions. Upward deflections denote rightward version. Error bars,  $\pm$ SE; subject, DY.

strongly favored the (leftward) motion in the test bands. The peak response is clearly offset slightly from zero, and the best-fit Gaussian function for these data (shown in continuous line) has an  $x$ -offset,  $\mu$ , of 0.41° (crossed disparity): this is our best estimate of the absolute disparity at which the rightward motion of the conditioning bands had their greatest influence on OFR. The width of the best-fit Gaussian,  $\sigma$ , was 0.55°, but the data show a slight asymmetry in the decay from the peak to the asymptote—there is a small undershoot with uncrossed disparities that is not seen with crossed disparities—that is not captured by the (symmetrical) Gaussian function. Nonetheless, the Gaussian function still provides a reasonable representation of the data, accounting for 97% of the disparity-related changes in OFR (i.e.,  $r^2 = 0.97$ ).

Fig. 1 also shows the disparity tuning curves obtained when crossed (circles and dotted line) and uncrossed (diamonds and dashed line) disparities of 1.6° were applied to the test bands. It is immediately evident that the major effect of applying disparity to the test bands was to shift the tuning curves upwards. If the dependence on the disparity of the conditioning bands had emanated solely from their disparity relative to the disparity of the

*test bands* then changes in the disparity of the test bands would have shifted the curves in Fig. 1 horizontally. More particularly, applying  $1.6^\circ$  of crossed disparity to the test bands would have shifted the curve  $1.6^\circ$  to the right and applying  $1.6^\circ$  of uncrossed disparity to the test bands would have shifted the curve  $1.6^\circ$  to the left. Based on the  $x$ -offset,  $\mu$ , of the best-fit Gaussian functions, the actual horizontal shifts were quite small ( $0.09^\circ$  and  $0.23^\circ$ , respectively) and rightward in both cases. The observed upward shift of the tuning curves indicates that OFR acquired a more rightward bias, consistent with the idea that applying disparity to the test bands reduces the impact of their (leftward) motion on OFR. The upward shift was much greater when the test bands had uncrossed disparity than when they had crossed disparity, the change in the  $y$ -offset,  $A$ , of the best-fit Gaussian functions being  $0.066^\circ$  and  $0.026^\circ$  in the two cases. To give these  $y$ -offsets some perspective, we expressed them as a percentage of the amplitude of the best-fit Gaussian (given by the difference between the peak and the asymptote) in the case in which the test disparity was zero. When so expressed, the changes in the  $y$ -offsets when the test bands were crossed and uncrossed amounted to 22% and 56%, respectively.

The data obtained with the opposite combination of motion stimuli—rightward test motion and leftward conditioning motion—showed very similar effects (though with the opposite sign, of course) and this is apparent from the parameters of the best-fit Gaussian functions listed for subject DY in Table 1.

### 3.2. Population data

Table 1 also lists the parameters of the best-fit Gaussian functions for three additional subjects who showed very similar trends. These Gaussian fits generally provided a very good representation of the disparity tuning curves, the  $r^2$  values ranging from 0.90 to 0.98 (mean  $\pm$  SD,  $0.96 \pm 0.03$ ), so that, on average, the fits accounted for 96% of the disparity-related variance.

That changing the absolute disparity of the test bands induced very little horizontal shift in the disparity tuning curves is evident from Fig. 2A, which shows the dependence of the  $x$ -offsets ( $\mu$ ) of the best-fit Gaussian functions on the absolute disparity applied to the test bands for all four subjects. If the  $x$ -offsets had been determined by the disparity of the conditioning bands *relative to the disparity of the test bands* then the curves in Fig. 2A would have had a slope of one (like the dashed line). Regression lines fitted to the data in Fig. 2A had positive slopes ranging from 0.01 to 0.18 (mean  $\pm$  SD,  $0.06 \pm 0.05$ ), indicating that, on average, the modulation of the  $x$ -offset with the disparity of the test bands was only  $\sim 6\%$  of that expected of a relative-disparity mechanism: for a complete list of these slopes, see the column labeled, “slope:  $\mu$  vs.  $d_t$ ”, in Table 1.

Although the mean  $x$ -offset when the test disparity was crossed was significantly greater (i.e., more crossed) than when the test disparity was uncrossed ( $p < 0.05$ , Student's  $t$ -test), the difference was only  $0.17^\circ$ , which is  $\sim 5\%$  of the difference in the test disparities.

Applying disparity to the test bands invariably shifted the OFR bias in favor of the motion in the conditioning bands, the  $y$ -offset of the best-fit Gaussians becoming more positive when the conditioning motion was rightward (as in Fig. 1) and more negative when the conditioning motion was leftward: see Table 1 and Fig. 3. The average  $y$ -offset, expressed with respect to the amplitude of the best-fit Gaussian when the test disparity was zero, was  $65\% \pm 26\%$  (SD). The effects on the width and amplitude of the best-fit Gaussians of applying disparity to the test bands were less consistent: four curves showed reduced width (mean reduction  $\pm$  SD,  $9\% \pm 9\%$ ) while the remainder (12) showed increased width (mean increase  $\pm$  SD,  $20\% \pm 20\%$ ), and four curves showed reduced amplitude (mean reduction  $\pm$  SD,  $14\% \pm 18\%$ ) while the remainder showed increased amplitude (mean increase  $\pm$  SD,  $31\% \pm 20\%$ ). See Table 1 for a complete listing of the widths ( $\sigma$ ) and amplitudes ( $P - A$ ).

### 3.3. Vergence eye movements

A major concern was the possibility that changing the disparity of the test bands resulted in changes in the vergence angle that significantly altered the absolute disparities experienced by the observer (though, of course, *not* the relative disparities). To address this question, we measured the average vergence angle over the 83-ms periods immediately following the onsets of the OFR stimuli, which approximated the periods during which the visual system was sampling the stimulus motions giving rise to our measured OFR, and computed the mean of these measures for all of the trials for each stimulus condition. Vergence showed very little within-subject variation in the various conditions: for a given subject, the total range of mean vergence angles never exceeded  $0.07^\circ$ , which is only  $\sim 2\%$  of the range of the applied test disparities ( $3.2^\circ$ ). This is evident from Fig. 4, which shows the dependence of the mean vergence angle on the disparity applied to the conditioning bands for each of the three test disparities used (for all four subjects). More particularly, the mean vergence angle when the test disparity was crossed exceeded that when the test disparity was uncrossed on average by only  $0.017^\circ$ , which is 0.5% of the difference in the applied test disparities: for a complete listing see the column in Table 1 labeled, “mean difference in vergence angle”. Thus, over the time period of interest, the vergence angle showed little dependence on the disparity applied to the test bands.

The estimated vergence errors—based on the difference between the mean vergence angles and the vergence

Table 1  
Dependence of the OFR on the disparity of the conditioning bands (parameters of the least-squares best-fit Gaussian functions): sensitivity to the disparity of the test bands

Subj	Motion	Test disparity $d_t$	$y$ -offset $A$	Scale factor $g$	Width $\sigma$	$x$ -offset $\mu$	Peak $P$	Amplitude $P - A$	$r^2$	Range of $N$	Mean difference in vergence angle	Slope: $\mu$ vs. $d_t$
FM	Test leftward Cond rightward	Uncrossed	0.023	0.337	0.86	0.07	0.179	0.156	0.98	166–174	0.015*	0.18 (0.18)
		Zero	-0.085	0.198	0.55	0.11	0.058	0.142	0.92	172–176		
		Crossed	-0.023	0.192	0.88	0.65	0.064	0.087	0.94	164–175		
	Test rightward Cond leftward	Uncrossed	0.188	-0.533	1.02	0.55	-0.020	-0.208	0.96	166–175	0.017*	0.06 (0.07)
		Zero	0.311	-0.344	0.98	0.80	0.171	-0.140	0.92	167–177		
		Crossed	0.162	-0.235	0.77	0.76	0.041	-0.121	0.91	163–177		
DY	Test leftward Cond rightward	Uncrossed	-0.059	0.250	0.75	0.49	0.073	0.132	0.99	123–137	0.015*	0.05 (0.04)
		Zero	-0.125	0.184	0.63	0.41	-0.008	0.117	0.97	126–138		
		Crossed	-0.099	0.237	0.72	0.64	0.033	0.132	0.98	126–135		
	Test rightward Cond leftward	Uncrossed	0.057	-0.225	0.71	0.63	-0.069	-0.126	0.99	127–136	0.005	0.06 (0.07)
		Zero	0.136	-0.152	0.67	0.56	0.045	-0.091	0.95	129–138		
		Crossed	0.098	-0.233	0.70	0.82	-0.035	-0.133	0.99	127–134		
BS	Test leftward Cond rightward	Uncrossed	-0.113	0.401	0.98	-0.19	0.051	0.164	0.97	69–76	0.019*	0.02 (0.01)
		Zero	-0.181	0.342	0.92	-0.41	-0.033	0.148	0.99	69–79		
		Crossed	-0.110	0.439	0.90	-0.13	0.086	0.196	0.99	70–76		
	Test rightward Cond leftward	Uncrossed	0.106	-0.434	1.08	-0.04	-0.054	-0.160	0.95	69–81	0.024*	0.02 (0.02)
		Zero	0.162	-0.308	0.77	-0.28	0.002	-0.160	0.96	69–80		
		Crossed	0.071	-0.368	0.83	0.04	-0.105	-0.176	0.98	69–79		
NB	Test leftward Cond rightward	Uncrossed	0.001	0.204	0.82	0.34	0.100	0.099	0.90	74–82	0.022*	0.01 (0.01)
		Zero	-0.085	0.187	0.73	0.00	0.017	0.102	0.99	74–82		
		Crossed	-0.026	0.275	0.79	0.36	0.112	0.138	0.98	75–82		
	Test rightward Cond leftward	Uncrossed	0.072	-0.179	0.64	0.23	-0.040	-0.112	0.96	75–81	0.021*	0.04 (0.03)
		Zero	0.144	-0.118	0.66	-0.04	0.073	-0.071	0.92	75–81		
		Crossed	0.077	-0.170	0.60	0.35	-0.037	-0.114	0.95	74–81		

The Gaussian function in Expression (1) was fitted to plots like those in Fig. 1, each plot having 13 data points, which were the means of multiple samples (*Range of N*, range of samples used for each mean); the parameters of these fits are given by  $A$ ,  $\sigma$ ,  $\mu$ ,  $P$  and  $P - A$ , which are in degrees, and  $g$ , which is dimensionless. *Mean difference in vergence angle*, a mean pre-response vergence angle was first computed by averaging the vergence angles over the time period 0–83 ms (from onset of stimulus motion) for all 13 conditioning disparities for each value of  $d_t$ , then the mean pre-response vergence angle when  $d_t$  was uncrossed was subtracted from the mean pre-response vergence angle when  $d_t$  was crossed. Slope:  $\mu$  vs.  $d_t$ , gives the slopes of the linear regression of  $x$ -offset ( $\mu$ ) on the disparity of the test bands ( $d_t$ ); values in parentheses were obtained after adjusting the disparities for any vergence error.

\*  $p < 0.05$  (Student's  $t$ -test).

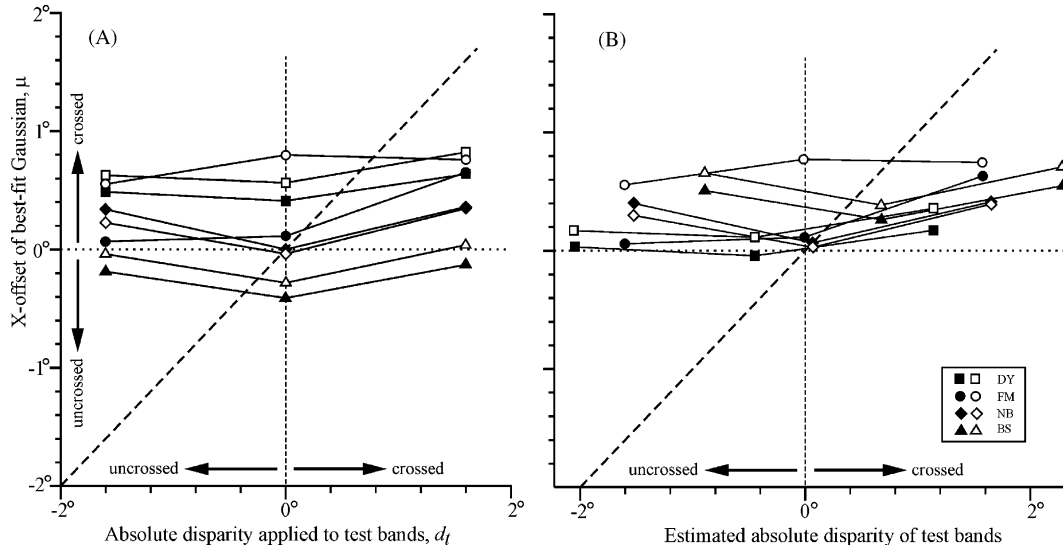


Fig. 2. Dependence of the x-offset of the best-fit Gaussian functions ( $\mu$ ) on the absolute disparity of the test bands ( $d_t$ ). (A) Before correction for vergence errors. (B) After correction for vergence errors. Sign convention, crossed disparities are positive. Filled symbols, leftward test motion and rightward conditioning motion. Open symbols, rightward test motion and leftward conditioning motion. Subjects: squares, DY; circles, FM; diamonds, NB; triangles, BS.

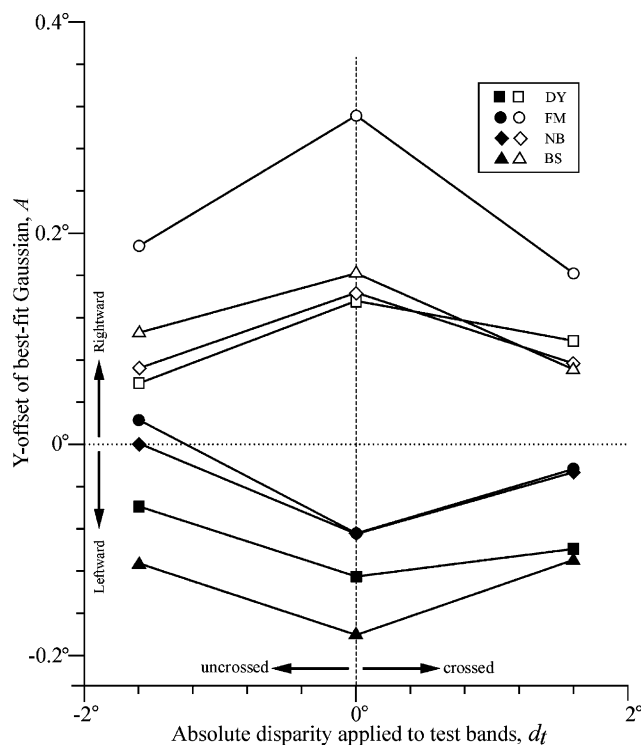


Fig. 3. Dependence of y-offset of best-fit Gaussian functions ( $A$ ) on the absolute disparity applied to the test bands ( $d_t$ ). Sign convention, rightward y-offsets and crossed disparities are positive. Filled symbols, leftward test motion and rightward conditioning motion. Open symbols, rightward test motion and leftward conditioning motion. Subjects: squares, DY; circles, FM; diamonds, NB; triangles, BS.

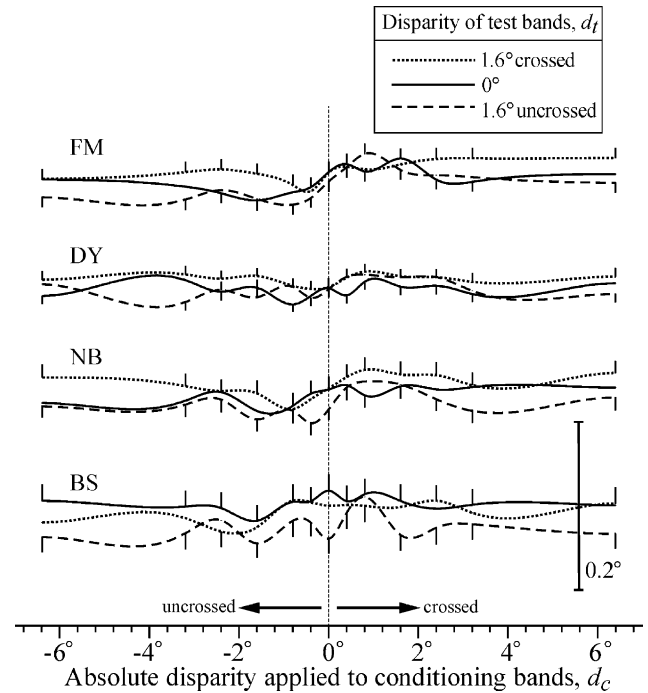


Fig. 4. Dependence of vergence angle on the disparity applied to the conditioning and test bands. The mean vergence position (in degrees), averaged over the 83-ms time period starting with the onset of the OFR stimuli, is plotted against the absolute disparity applied to the conditioning bands ( $d_c$ , in degrees). The data for both directions of stimulus motion (leftward test/rightward conditioning; rightward test/leftward conditioning) have been pooled. The absolute disparity of the test bands ( $d_t$ ) was zero (continuous lines),  $1.6^\circ$  crossed (dotted lines), and  $1.6^\circ$  uncrossed (dashed lines). Curves are cubic spline interpolations. Upward deflections denote increased vergence. Error bars, 1 SE.

angle required to align the two eyes on the center of the screen as indicated by our calibration procedure—varied substantially between subjects: FM and DY were gen-

erally overconverged (overall mean vergence error for all conditions  $\pm$  SD:  $0.02^\circ \pm 0.03^\circ$  and  $0.45^\circ \pm 0.09^\circ$ ,

respectively), while NB and BS were generally under-converged ( $0.07^\circ \pm 0.05^\circ$  and  $0.69^\circ \pm 0.07^\circ$ , respectively). The vergence errors provided estimates of the fixation disparities and so allowed us to also estimate the absolute disparities actually experienced by the subject at the screen center. Using these adjusted values we replotted the disparity tuning curves, fitted each with a Gaussian function and then plotted their  $x$ -offsets against the estimated mean absolute test disparity: see Fig. 2B. (Note that the estimated absolute disparities of the test bands in Fig. 2B were each based on the mean vergence error for *all* 13 conditioning disparities for each combination of stimulus motions). A comparison of Fig. 2A and B indicates that the major effect on the  $x$ -offsets of compensating for the vergence errors was to reduce the inter-subject vertical scatter (slightly) and to increase the inter-subject horizontal scatter. We saw in Fig. 4 that there was little within-subject variation in the vergence angle so it is perhaps not surprising that the slopes of the least-squares best fit linear regressions for the data in Fig. 2B never differed from those for the corresponding data in Fig. 2A by more than 1%. These slopes are listed in parentheses in the column labeled, “Slope:  $\mu$  vs.  $d_t$ ”, in Table 1, and ranged from 0.01 to 0.18 (mean  $\pm$  SD,  $0.05 \pm 0.06$ ), indicating that, after compensating for vergence errors, on average the modulation of the  $x$ -offset with the disparity of the test bands was only  $\sim 5\%$  of that expected of a relative-disparity mechanism. These values are almost identical to those obtained without compensation for vergence errors. Thus, the very small positive slopes in Fig. 2A were not secondary to changes in the vergence angle. Other parameters of the best-fit Gaussian functions ( $y$ -offset, peak, amplitude) never changed by more than 1% when vergence errors were compensated. In sum, changes in the vergence angle were minor and had negligible impact on the OFR data.

#### 4. Discussion

A previous study on humans reported that binocular disparity applied uniformly to a large random-dot pattern had a relatively minor effect on the initial OFR elicited by motion of that pattern, but when the pattern was partitioned into regions with conflicting motion then altering the disparity of one of those regions could have a substantial impact on initial net tracking (Masson et al., 2001). In particular, when the pattern was subdivided into two interleaved sets of horizontal bands of test and conditioning dots that suddenly underwent horizontal motion in opposite directions, applying disparity to the conditioning dots substantially reduced their impact so that the initial OFR was now dominated by the motion of the test dots that remained in the plane of fixation. The suggestion was made that the initial

OFR relied on motion detectors that were sensitive to relative motion and/or relative disparity. The present experiments have replicated these previous findings with partitioned dot patterns and shown that the disparity tuning curves describing the dependence on the disparity of the conditioning pattern are well fit by a Gaussian function whose  $x$ -offset is usually close to zero disparity. We reasoned that if a relative disparity mechanism were involved then a change in the disparity of the test dots should result in an equal change in this  $x$ -offset. However, we now report that the changes in  $x$ -offset were on average only 5–6% of the applied changes in the disparity of the test pattern (Fig. 2), indicating that the system was almost exclusively sensitive to the absolute disparity. There were consistent, often appreciable, changes in the  $y$ -offset—applying disparity to the test bands invariably shifted the OFR bias in favor of the motion in the conditioning bands—but this was to be expected, at least in part, from the reduced efficacy of the test bands when given disparity.

We conclude from these experiments that initial OFR is sensitive to absolute disparity and, as a consequence, is much more responsive to objects moving in the vicinity of the plane of fixation than to objects moving—often with competing motion—in other depth planes. The dependence on absolute disparity means that ocular following functions in harmony with disparity vergence, which is known to use absolute disparity to bring objects of interest into the plane of fixation (Busettoni et al., 2001; Erkelens & Collewijn, 1985a; Westheimer & Mitchell, 1956).

The  $x$ -offset of the best-fit Gaussian functions, indicating the absolute disparity at which the conditioning stimulus had its greatest impact, was generally not located exactly at zero and even after compensating for the vergence errors in our experiment tended to be slightly shifted towards crossed disparities (Fig. 2B). We suggest that this was at least in part a consequence of our using a tangent screen and referring all absolute disparities to the screen center, which has crossed disparity relative to eccentric locations on the screen. If the ocular following mechanism integrates motion inputs over a wide area (extent presently unknown) and has indeed a preference for zero absolute disparity then, in our experimental situation, a certain amount of crossed disparity would be needed at the center to offset the uncrossed disparities at eccentric locations. Other studies that used a tangent screen to examine the tolerance of short-latency vertical disparity-vergence responses for horizontal disparity also found a slight crossed-disparity bias and attributed this to a similar cause (Yang, Fitz-Gibbon, & Miles, 2003).

It is well known that human stereopsis—depth perception based on binocular stereo cues—is much better for relative disparity than for absolute disparity (Erkelens & Collewijn, 1985a, 1985b; Kumar & Glaser, 1992;



Regan, Erkelens, & Collewijn, 1986; Westheimer, 1979) and the same is true of monkeys (Prince, Pointon, Cumming, & Parker, 2000). Thus, our finding that the disparity mechanisms influencing the initial short-latency OFR depend on absolute rather than relative disparity is consistent with the idea that these ultra-rapid responses—like those responsible for the initial short-latency disparity vergence (Masson, Busetini, & Miles, 1997)—operate independently of perception and perhaps occur before the observer is even aware that there has been a visual disturbance (Miles, 1998).

Monkeys provide a valuable animal model for studying the initial OFR, sharing many properties with humans (Gellman et al., 1990; Kawano & Miles, 1986; Miles et al., 1986), and also have excellent binocular vision. Disparity-sensitive neurons have been recorded in several regions of the monkey's cortex, some of which are of particular interest to us here because they contain cells that are sensitive to both motion and binocular disparity. These include the medial temporal area (MT) (Bradley & Andersen, 1998; Bradley, Qian, & Andersen, 1995; DeAngelis, Cumming, & Newsome, 1998; DeAngelis & Newsome, 1999; Maunsell & Van Essen, 1983b) and the medial superior temporal area (MST) (Eifuku & Wurtz, 1998; Roy, Komatsu, & Wurtz, 1992), which receives major inputs from MT (Maunsell & Van Essen, 1983a; Ungerleider & Desimone, 1986; Van Essen, Maunsell, & Bixby, 1981) and has been strongly implicated in the generation of the initial OFR (Kawano, Shidara, Watanabe, & Yamane, 1994; Takemura, Inoue, & Kawano, 2002). Unfortunately, few studies have attempted to determine whether the cells in these regions are specialized for sensing absolute or relative disparity. Recent neurophysiological studies have concluded that most disparity-sensitive cells in cortical areas V1 (Cumming & Parker, 1999) and MT (Uka & DeAngelis, 2002) are responsive to absolute disparity because the preferred disparity in the receptive field centers is generally independent of the disparity in the surround regions. In fact, to date, only cortical region V2 has been shown to contain cells whose preferred disparities in the center of the receptive field are strongly dependent on the disparity in the surround, the hallmark of a mechanism sensing relative disparity (Thomas, Cumming, & Parker, 2002). However, it is not clear that the sensing of relative disparity necessarily always involves center/surround comparisons and other spatial configurations need to be explored. Eifuku and Wurtz (1999) suggested that some motion-sensitive neurons in MST were selectively sensitive to relative disparity because the optimal disparities for the centers and surrounds of their receptive fields were different (Bradley & Andersen, 1998; Eifuku & Wurtz, 1999) but, as pointed out by Cumming and DeAngelis (2001) and Thomas et al. (2002), such neurons might merely be differentially sensitive to absolute disparity in their centers and surrounds.

The observation of Masson et al. (2001) that the effects of disparity on initial OFR were much greater when the disparity was applied selectively to regional elements with conflicting motion than when applied uniformly to the whole display led them to suggest that image segmentation mechanisms were operating. Motion signals are known to facilitate scene segmentation (Braddick, 1993; Nakayama, 1985; Stoner & Albright, 1993) and the opponent center-surround organization of the receptive fields of some cells in MT and MST—in which the center and surround prefer opposite directions of motion—has been invoked as the neural basis for this (Allman, Miezin, & McGuinness, 1985a, 1985b; Born, Groh, Zhao, & Lukasewycz, 2000; Bradley & Andersen, 1998; Eifuku & Wurtz, 1998; Tanaka et al., 1986). Some of these cells are disparity sensitive and have a preference for zero disparity (Bradley & Andersen, 1998), exactly the sort of properties that might be expected of cells mediating the strongly disparity-dependent OFR when there is conflicting motion. However, such neurons are poorly responsive to coherent large-field motion, which is a powerful stimulus for OFR even when the images have disparity. Thus, the OFR elicited with large uniform patterns would seem to require neurons with much weaker inhibitory surrounds and a more modest preference for zero disparity. These seemingly different properties might define the two ends of a continuum of cells mediating OFR, cf., the population coding of disparity vergence in MST (Takemura, Inoue, Kawano, Quaia, & Miles, 2001).

### Acknowledgements

We thank Tom Ruffner, Nick Nichols, and Lee Jensen for technical assistance, Ed Fitzgibbon, John McClurkin, Kelvin Chen and Art Hays for software support, Jean Steinberg for secretarial assistance, and our subjects for their patience.

### References

- Allman, J., Miezin, F., & McGuinness, E. (1985a). Direction- and velocity-specific responses from beyond the classical receptive field in the middle temporal visual area (MT). *Perception*, *14*, 105–126.
- Allman, J., Miezin, F., & McGuinness, E. (1985b). Stimulus specific responses from beyond the classical receptive field: neurophysiological mechanisms for local–global comparisons in visual neurons. *Annual Review of Neuroscience*, *8*, 407–430.
- Born, R. T., Groh, J. M., Zhao, R., & Lukasewycz, S. J. (2000). Segregation of object and background motion in visual area MT: effects of microstimulation on eye movements. *Neuron*, *26*, 725–734.
- Braddick, O. (1993). Segmentation versus integration in visual motion processing. *Trends in Neuroscience*, *16*, 263–268.
- Bradley, D. C., & Andersen, R. A. (1998). Center-surround antagonism based on disparity in primate area MT. *The Journal of Neuroscience*, *18*, 7552–7565.

- Bradley, D. C., Qian, N., & Andersen, R. A. (1995). Integration of motion and stereopsis in middle temporal cortical area of macaques. *Nature*, *373*, 609–611.
- Busettoni, C., FitzGibbon, E. J., & Miles, F. A. (2001). Short-latency disparity vergence in humans. *Journal of Neurophysiology*, *85*, 1129–1152.
- Collewijn, H., Van Der Mark, F., & Jansen, T. C. (1975). Precise recording of human eye movements. *Vision Research*, *15*, 447–450.
- Cumming, B. G., & DeAngelis, G. C. (2001). The physiology of stereopsis. *Annual Review Neuroscience*, *24*, 203–238.
- Cumming, B. G., & Parker, A. J. (1999). Binocular neurons in V1 of awake monkeys are selective for absolute, not relative, disparity. *The Journal of Neuroscience*, *19*, 5602–5618.
- DeAngelis, G. C., Cumming, B. G., & Newsome, W. T. (1998). Cortical area MT and the perception of stereoscopic depth. *Nature*, *394*, 677–680.
- DeAngelis, G. C., & Newsome, W. T. (1999). Organization of disparity-selective neurons in macaque area MT. *The Journal of Neuroscience*, *19*, 1398–1415.
- Eifuku, S., & Wurtz, R. H. (1998). Response to motion in extrastriate area MSTl: center-surround interactions. *Journal of Neurophysiology*, *80*, 282–296.
- Eifuku, S., & Wurtz, R. H. (1999). Response to motion in extrastriate area MSTl: disparity sensitivity. *Journal of Neurophysiology*, *82*, 2462–2475.
- Erkelens, C. J., & Collewijn, H. (1985a). Eye movements and stereopsis during dichoptic viewing of moving random-dot stereograms. *Vision Research*, *25*, 1689–1700.
- Erkelens, C. J., & Collewijn, H. (1985b). Motion perception during dichoptic viewing of moving random-dot stereograms. *Vision Research*, *25*, 583–588.
- Eubank, R. L. (1988). Spline smoothing and nonparametric regression. In D. B. Owen (Ed.), *Statistics: textbooks and monographs, Vol. 90*. New York: Marcel Dekker.
- Gellman, R. S., Carl, J. R., & Miles, F. A. (1990). Short latency ocular-following responses in man. *Visual Neuroscience*, *5*, 107–122.
- Hays, A. V., Richmond, B. J., & Optican, L. M. (1982). A UNIX-based multiple process system for real-time data acquisition and control. *WESCON conference proceedings* (pp. 1–10), Vol. 2.
- Howard, I. P., & Gonzalez, E. G. (1987). Human optokinetic nystagmus in response to moving binocularly disparate stimuli. *Vision Research*, *27*, 1807–1816.
- Howard, I. P., & Simpson, W. A. (1989). Human optokinetic nystagmus is linked to the stereoscopic system. *Experimental Brain Research*, *78*, 309–314.
- Kawano, K., & Miles, F. A. (1986). Short-latency ocular following responses of monkey. II. Dependence on a prior saccadic eye movement. *Journal of Neurophysiology*, *56*, 1355–1380.
- Kawano, K., Shidara, M., Watanabe, Y., & Yamane, S. (1994). Neural activity in cortical area MST of alert monkey during ocular following responses. *Journal of Neurophysiology*, *71*, 2305–2324.
- Kumar, T., & Glaser, D. A. (1992). Depth discrimination of a line is improved by adding other nearby lines. *Vision Research*, *32*, 1667–1676.
- Mackensen, G. (1953). Untersuchungen zur Physiologie des optokinetischen Nystagmus. *Klinische Monatsblätter für Augenheilkunde*, *123*, 133–143.
- Masson, G. S., Busettini, C., & Miles, F. A. (1997). Vergence eye movements in response to binocular disparity without depth perception. *Nature*, *389*, 283–286.
- Masson, G. S., Busettini, C., Yang, D.-S., & Miles, F. A. (2001). Short-latency ocular following in humans: sensitivity to binocular disparity. *Vision Research*, *41*, 3371–3387.
- Maunsell, J. H., & Van Essen, D. C. (1983a). The connections of the middle temporal visual area (MT) and their relationship to a cortical hierarchy in the macaque monkey. *The Journal of Neuroscience*, *3*, 2563–2586.
- Maunsell, J. H., & Van Essen, D. C. (1983b). Functional properties of neurons in middle temporal visual area of the macaque monkey. II. Binocular interactions and sensitivity to binocular disparity. *Journal of Neurophysiology*, *49*, 1148–1167.
- Miles, F. A. (1998). The neural processing of 3-D visual information: evidence from eye movements. *The European Journal of Neuroscience*, *10*, 811–822.
- Miles, F. A., Kawano, K., & Optican, L. M. (1986). Short-latency ocular following responses of monkey. I. Dependence on temporospatial properties of visual input. *Journal of Neurophysiology*, *56*, 1321–1354.
- Nakayama, K. (1985). Biological image motion processing: a review. *Vision Research*, *25*, 625–660.
- Prince, S. J., Pointon, A. D., Cumming, B. G., & Parker, A. J. (2000). The precision of single neuron responses in cortical area V1 during stereoscopic depth judgments. *The Journal of Neuroscience*, *20*, 3387–3400.
- Regan, D., Erkelens, C. J., & Collewijn, H. (1986). Necessary conditions for the perception of motion in depth. *Investigative Ophthalmology and Visual Science*, *27*, 584–597.
- Robinson, D. A. (1963). A method of measuring eye movement using a scleral search coil in a magnetic field. *IEEE Transactions on Biomedical Engineering, BME-10*, 137–145.
- Roy, J. P., Komatsu, H., & Wurtz, R. H. (1992). Disparity sensitivity of neurons in monkey extrastriate area MST. *The Journal of Neuroscience*, *12*, 2478–2492.
- Stoner, G. R., & Albright, T. D. (1993). Image segmentation cues in motion processing: Implications for modularity in vision. *Journal of Cognitive Neuroscience*, *5*, 129–149.
- Takemura, A., Inoue, Y., & Kawano, K. (2002). Visually driven eye movements elicited at ultra-short latency are severely impaired by MST lesions. *Annals of the New York Academy of Sciences*, *956*, 456–459.
- Takemura, A., Inoue, Y., Kawano, K., Quaia, C., & Miles, F. A. (2001). Single-unit activity in cortical area MST associated with disparity-vergence eye movements: evidence for population coding. *Journal of Neurophysiology*, *85*, 2245–2266.
- Tanaka, K., Hikosaka, K., Saito, H., Yukie, M., Fukada, Y., & Iwai, E. (1986). Analysis of local and wide-field movements in the superior temporal visual areas of the macaque monkey. *The Journal of Neuroscience*, *6*, 134–144.
- Thomas, O. M., Cumming, B. G., & Parker, A. J. (2002). A specialization for relative disparity in V2. *Nature Neuroscience*, *5*, 472–478.
- Uka, T., & DeAngelis, G. C. (2002). MT neurons do not signal relative disparity. *Journal of Vision*, *2*(7), 37a, Available: <http://journalofvision.org/2/7/37/>.
- Ungerleider, L. G., & Desimone, R. (1986). Cortical connections of visual area MT in the macaque. *The Journal of Comparative Neurology*, *248*, 190–222.
- Van Essen, D. C., Maunsell, J. H., & Bixby, J. L. (1981). The middle temporal visual area in the macaque: myeloarchitecture, connections, functional properties and topographic organization. *The Journal of Comparative Neurology*, *199*, 293–326.
- Westheimer, G. (1979). Cooperative neural processes involved in stereoscopic acuity. *Experimental Brain Research*, *36*, 585–597.
- Westheimer, G., & Mitchell, A. M. (1956). Eye movement responses to convergent stimuli. *Archives of Ophthalmology*, *55*, 848–856.
- Yang, D.-S., FitzGibbon, E. J., & Miles, F. A. (2003). Short-latency disparity-vergence eye movements in humans: sensitivity to simulated orthogonal tropias. *Vision Research*, *43*, 431–443.